World Scientific
www.worldscientific.com

REGIOSELECTIVITY INVESTIGATION FOR THE PYROLYSIS OF XANTHATES: A COMPUTATIONAL STUDY

PING WU

*Key Laboratory of Coordination Chemistry
and Functional Materials in Universities of Shandong
Dezhou College, Dezhou, Shandong 253023, P. R. China
pingwu.dzu@gmail.com*

JOHNNY TRUONG

*Department of Chemistry
Georgia State University, Atlanta, GA 30319, USA
jtruong1992@gmail.com*

YONGSHUN HUANG*

*Department of Chemistry
University of Cincinnati, Cincinnati, OH 45221, USA
hyshun.pig@gmail.com*

JIAXING LI*

*Key Laboratory of Novel Thin Film Solar Cells
Institute of Plasma Physics
Chinese Academy of Sciences, Hefei
Anhui 230031, P. R. China
lijx@ipp.ac.cn*

MP2/6-31+G(d,p)//MP2/6-31G(d) method was employed to investigate the pyrolyses of O-*sec*-butyl S-methyl xanthate (Chugeav reaction) and S-*sec*-butyl O-methyl xanthate, which gave regioselective products of E-butene, Z-butene and 1-butene. Both procedures were found to have 13 possible pathways, of which nine pathways would generate the alkene products. For O-*sec*-butyl S-methyl xanthate, the computational results indicated that the most favorable three pathways corresponded to a two-step mechanism, with the rate-determining step to be a thion sulfur atom involved six-membered ring transition states. The calculated products distribution was consistent with the experimental observations. However, for S-*sec*-butyl O-methyl xanthate, thiol-participated four-membered ring transition states were found to be more energetically favored than the six-membered ring transition state to produce 1-butene, which can be attributed to a larger sulfur atomic size than an oxygen atom. As the calculation result,

*Corresponding authors.

only trace amount of 1-butene could be obtained with a major product being E-butene and Z-butene as a minority.

1. Introduction

As a valuable synthetic route to synthesize alkenes without rearrangement of the carbon skeleton, pyrolysis of xanthate precursors was first reported by L. Chugeav in 1899 in their studies on the optical properties of xanthates.[1,2] This method had attracted considerable interests in polymer chemistry for the synthesis of poly-paraphenylene-vinylene (PPV) samples, which had applied as promising character-istics for fabrication of light-emitting devices.[3–6]

Xanthates can be easily prepared by the reaction of the corresponding alcohols with a base and carbon disulfide, followed by trapping with an alkyl iodide (usually methyl iodide).[7] At least one β-hydrogen of the xanthate is required to ensure that the pyrolysis will lead to the alkenes, together with the elimination of by-products (carbonyl sulfide and a thiol). However, if more than one β-hydrogen is present, regioselectivity will need to be considered, which will limit the application of the Chugeav reaction. Xanthates with no β-hydrogen will undergo thione-to-thiol rearrangements, giving S,S-dialkyl dithiocarbonates (Scheme 1).

The mechanism of the Chugeav reaction was proposed to involve two possible pathways (Scheme 2). The first pathway reacts in a one-step mechanism, yielding an alkene, a carbonyl sulfide and a thiol. In the second mechanism, a thione group, rather than a thiol group, will attack the β-hydrogen, giving an alkene and an
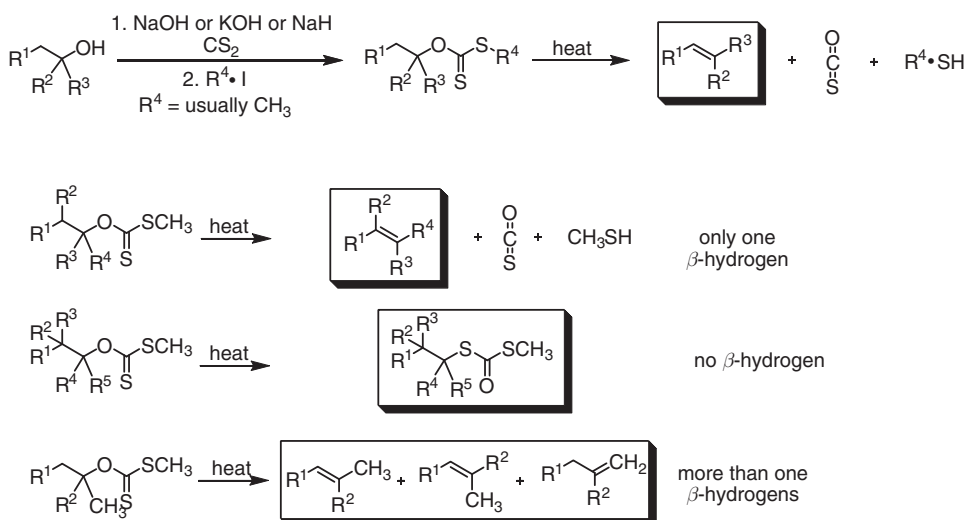
Scheme 1.   Chugeav reaction with different β-hydrogens.
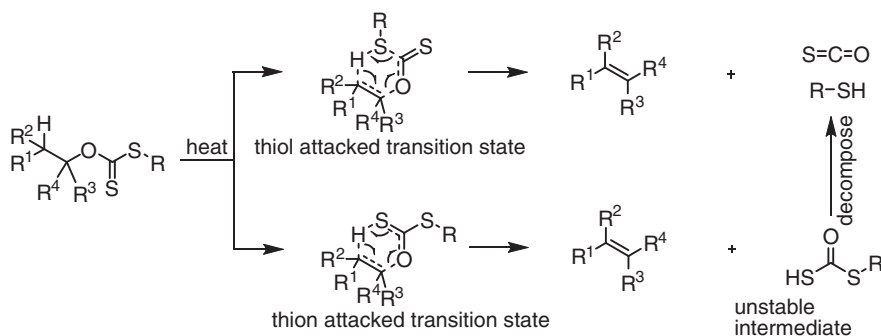
Scheme 2. Two proposed mechanisms for the pyrolysis of xanthates.

unstable S-alkyl dithiocarbonate intermediate, which will decompose to carbonyl sulfide and a thiol. The first pathway was supported by W. Hückel in 1940,[8] while D. H. Barton[9] and D. J. Cram[10] preferred the second mechanism. Experimental studies were also applied to investigate the Chugeav mechanisms. Alexander and Mudrak proved the *cis*-elimination mechanism.[11–13] Bader and Bourns[14] made isotope effect studies for the pyrolysis of *trans*-2-methyl-1-indanyl xanthate and found solid evidence for the second pathway and further kinetic and thermodynamic studies concluded that the Chugeav reactions were homogenous and unimolecular.

As for the theoretical studies, Erickson and Kahn[15] first calculated the activation energies of HSC(S)OEt at MP2/6-31G(d)//HF/6-31G(d) level in 1994. Deleuze group[16] investigated the E_i reaction of EtSC(S)OMe and its substituent effects (such as α-CN, β-CN, *trans*-stilbene and *cis*-stilbene) at different theoretical levels (HF, B3LYP, MPW1K, MP2, MP3, MP4, CCSD, CCSD(T)) and different basis sets (6-31G*, 6-31G**, 6-311G**, 6-311++G**, cc-pVDZ). In comparison with all these methods and basis sets, DFT calculations gave with longer or shorter bond lengths and underestimated the activation energies, whereas HF method tended to significantly overestimate the activation energy. However, MP2 barriers matched nicely with benchmark CCSD(T) activation energies. Harano[17] utilized B3LYP/6-31G(d) theoretical level to study the transition states of MeSC(S)OEt. Recently, Vélez group[18] considered five possible mechanisms for the thermal decomposition of a series of xanthates at the level of MP2/6-31G(d). Similar theoretical studies were also applied to the other computational systems.[19–23] However, all the previous studies focused on either the various computational methods or different transition states, none of them had considered the regioselectivity of the Chugeav reaction. As for the experimental results, Goeders group[24] pyrolyzed different xanthates by dropping into external heated glass columns. The products were collected by liquid nitrogen and analyzed by gas phase chromatography. The distributions of regioselective products were determined titrimetrically or gravimetrically. Of all the xanthates, O-*sec*-butyl S-methyl xanthate gave products of Z-butene, E-butene and 1-butene with a distribution ratio to be 40:19:14, after normalization (the original ratio is

40:19:41), which was also selected in this paper, together with S-*sec*-butyl O-methyl xanthate, to investigate the regioselectivity of the Chugeav reaction at the computational level of MP2/6-31+G(d,p)//MP2/6-31G(d).

2. Calculation Methods

All calculations were preformed with the help of Gaussian 03 package.[25] As mentioned by Deleuze group[16] that the MP2 level[26] gave nice activation barriers for the pyrolysis of xanthates as the CCSD(T) method, which was also applied by Vélez[18] with the basis set of 6-31G(d),[27] the same computational level was also selected for the structural optimization. For the transition state calculations, force constants were also calculated with MP2/6-31G(d) method and noeigentest was applied to facilitate the transition state optimization. A higher basis set of 6-31+G(d,p) was employed to calculate the single-point energy based on the optimized structures in order to obtain more accurate results. The frequency calculations were evaluated at 623.15 K, as the experimental temperature.[24] A scaling factor[28] of 0.9670 for the zero-point vibrational energies was used for correction. All zero-gradient structures were characterized by a vibrational analysis with no imaginary frequency. All of the transition-state structures had only one imaginary frequency, which was interpreted as a negative vibrational mode, and the intrinsic reaction coordinate (IRC)[29] was followed to make sure that each transition state connects the expected reactant and product.

Classic transition-state theory (TST)[30,31] was selected to calculate the relative rate constant, $k(T)$, for the rate-determining steps, which was also proportional to the product distributions. The equation is shown below, which assumes that the transmission coefficient is equal to unity:

$$k(T) = \frac{k_B T}{h} e^{\frac{-\Delta G^{\neq}(T)}{RT}},$$

where k_B, h and R are the Boltzmann constant, Planck's constant and the universal gas constant, respectively, and $\Delta G^{\neq}(T)$ is the standard free energy of activation at the absolute temperature T.

3. Results and Discussion

Five possible mechanisms had been calculated by Vélez group for the pyrolysis of O-alkyl (Et, *i*-Pr and *t*-Bu) S-methyl xanthates and S-alkyl (Et, *i*-Pr and *t*-Bu) O-methyl xanthates.[18] Of all the five mechanisms, only two mechanisms with six-membered ring transition states resulted in the desired alkene products, while ignoring that four-membered ring transition states could also give alkene products. Besides, five-membered ring transition states were also found to give ketones or thioketones. Herein, we presented a detailed mechanism study for the thermal decomposition of O-*sec*-butyl S-methyl xanthate and S-*sec*-butyl O-methyl xanthate.

3.1. *Pyrolysis of O-sec-butyl S-methyl xanthate*

The MP2/6-31+G(d,p)//MP2/6-31G(d) calculated results for the pyrolysis of O-*sec*-butyl S-methyl xanthate in the gas phase were shown in Schemes 3 and 4.

As can be seen from the schemes, 13 possible pathways were considered for the mechanism study, of which pathways A to I ended up with the Chugeav reaction products. In pathways A, B and E, a thion sulfur atom attacked a β-hydrogen *via* a six-membered ring transition state, giving the desired Z-butene, E-butene and 1-butene, together with an unstable intermediate, S-methyl dithiocarbonate (INT1), which rapidly decomposed into carbonyl sulfide and methanthiol. For pathways C, D and F, the same products would be obtained, but a thiol sulfur atom was participated with a one-step process. Besides a sulfur atom, an oxygen atom could also act as a nucleophile, as shown in pathways G, H and I, to extract a β-hydrogen atom through a four-membered ring transition state. Herein, S-methyl xanthate (INT2) was generated as an intermediate, which also pyrolyzed into methanthiol and carbonyl sulfide. Pathway J resulted in a thion-to-thiol rearrangement product, S-*sec*-butyl S-methyl dithiocarbonate (P-7). Pathways K and L gave off carbonyl sulfide and carbon disulfide, leaving *sec*-butyl methyl thioether (P-8) and *sec*-butyl methyl ether (P-9), respectively. Pathway M was revealed with a five-membered transition state
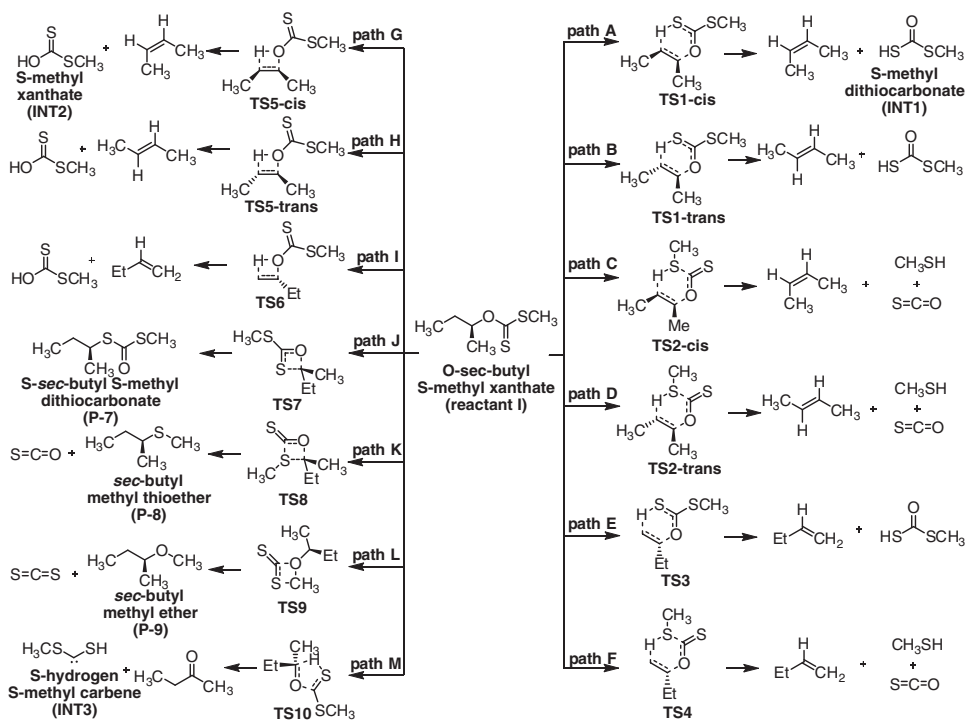
Scheme 3.   Thirteen possible pathways for the thermolysis of O-*sec*-butyl S-methyl xanthate.
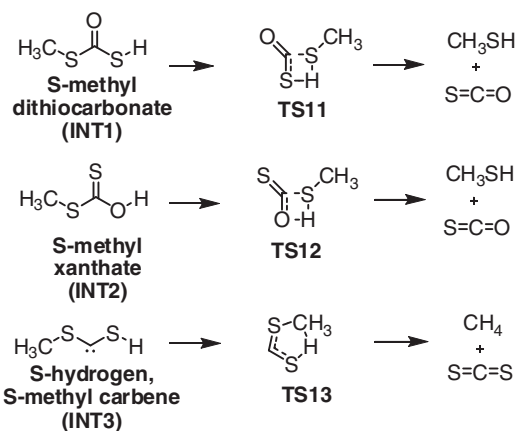
Scheme 4. Thermal decomposition of INT1, INT2 and INT3.

to give butanone and S-hydrogen S-methyl carbene (INT3), which was unstable and easily decomposed into methane and carbon disulfide.

The corrected Gibbs energies for the reactants, transition states and products involved in the pyrolysis of O-*sec*-butyl S-methyl xanthate were collected in Table 1 at MP2/6-31+G(d,p)//MP2/6-31G(d) level, while the detailed electronic energies, zero-point vibrational energies, thermal corrections to enthalpies, entropies and the calculation methods were displayed in Table S1 in the supporting information. The Gibbs free energy profiles for all pathways were depicted in Figs. 1 and 2.

According to Figs. 1 and 2, the lowest barriers for the pyrolysis of O-*sec*-butyl S-methyl xanthate corresponded to pathways B, A and E, all of which were exothermic pathways with late transition states of TS1-trans, TS1-cis and TS3. The activation energies for TS1-trans, TS1-cis and TS3 were 38.30, 39.65 and 40.54 kcal·mol^{-1}, respectively, with the differences of only 1.35 kcal·mol^{-1} (TS1-cis VS TS1-trans) and 0.89 kcal·mol^{-1} for TS3 *versus* TS1-cis. According to above

Table 1. Corrected Gibbs energies, in Hartrees, for the reactants, transition states and products involved in the pyrolysis of O-*sec*-butyl S-methyl xanthate at MP2/6-31+G(d,p)//MP2/6-31G(d).

| Species	Corrected G	Species	Corrected G	Species	Corrected G
reactant I	−1105.3364184	TS8	−1105.2376825	P-9	−272.0430996
TS1-cis	−1105.2732393	TS9	−1105.2123258	INT1	−948.6994613
TS1-trans	−1105.2753856	TS10	−1105.2222227	INT2	−948.6877888
TS2-cis	−1105.2548255	TS11	−948.6426505	INT3	−873.5555020
TS2-trans	−1105.2552343	TS12	−948.6279945	butanone	−231.7332780
TS3	−1105.2712175	TS13	−873.5104950	CH$_3$ OH	−115.3972433
TS4	−1105.2529187	*Z*-butene	−156.6593760	CH$_3$SH	−438.0027460
TS5-cis	−1105.2520597	*E*-butene	−156.6604383	CH$_4$	−40.3634193
TS5-trans	−1105.2537616	1-butene	−156.6560539	S=C=S	−833.3169485
TS6	−1105.2503782	P-7	−1105.3559477	O=C=S	−510.7380868
TS7	−1105.2591576	P-8	−594.6560415		
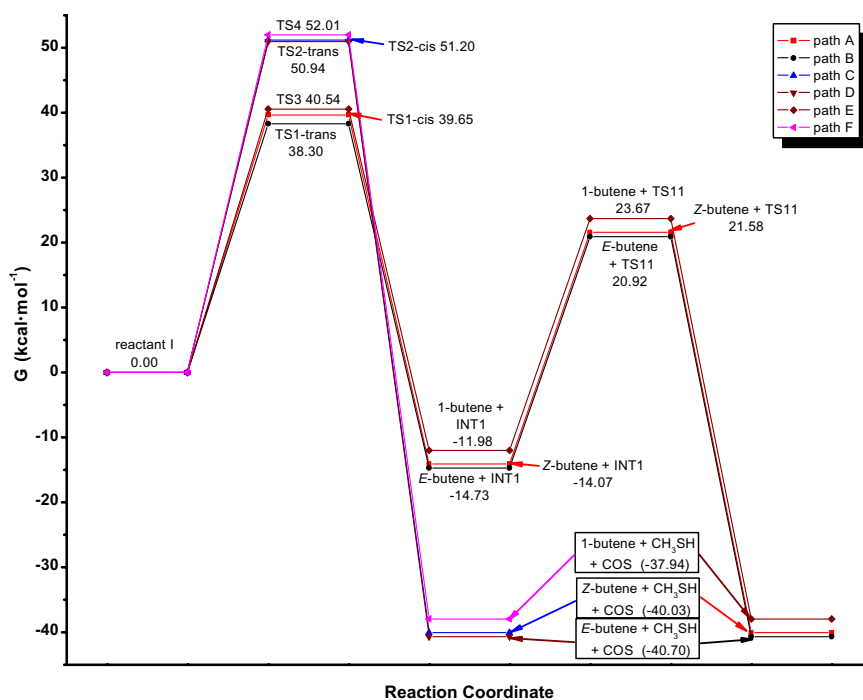
Fig. 1.   Gibbs energy profile of pathways A to F for the pyrolysis of O-*sec*-butyl S-methyl xanthate.

mentioned classic TST equation, the relative rate constants were calculated to be 40:13:7 for TS1-trans, TS1-cis and TS3. This theoretical result agreed with the experimental observation, of which three alkenes were measured to be 40:19:14 for E-butene, Z-butene and 1-butene after normalization.[24] All three transition states produced the corresponding alkene together with a same intermediate, S-methyl dithiocarbonate (INT1). INT1 would decompose into methanthiol and carbonyl sulfide *via* a four-membered ring transition state with the energy barrier to be $35.65 \, \text{kcal} \cdot \text{mol}^{-1}$. The reaction energies for the whole procedures were found to be -40.70, -40.03 and $-37.94 \, \text{kcal} \cdot \text{mol}^{-1}$, respectively, indicating that they were all exothermic.

For TS2-cis, TS2-trans and TS4 (Fig. 1), the corresponding activation energies raised to 51.20, 50.94 and $52.01 \, \text{kcal} \cdot \text{mol}^{-1}$, which was consistent with the experimental observation for the isotope effect of $^{32}\text{S}/^{34}\text{S}^{8}$ and clearly indicated that a thion sulfur atom was highly preferred over a thiol sulfur atom to attack a β-hydrogen. For the four-membered ring transition states (Fig. 2), TS5-cis, TS5-trans and TS6 had activation energies of 52.94, 51.87 and $53.99 \, \text{kcal} \cdot \text{mol}^{-1}$, resulting in Z-butene, E-butene, 1-butene and INT2. INT2 would convert to methanthiol and carbonyl sulfide *via* TS12 with a $37.52 \, \text{kcal} \cdot \text{mol}^{-1}$ energy barrier. TS7, TS8 and TS9 were similar transition states as E. Vélez group considered.[18] TS7 was $48.48 \, \text{kcal} \cdot \text{mol}^{-1}$ higher than reactant I, producing P-7. TS8 ($61.96 \, \text{kcal} \cdot \text{mol}^{-1}$) and
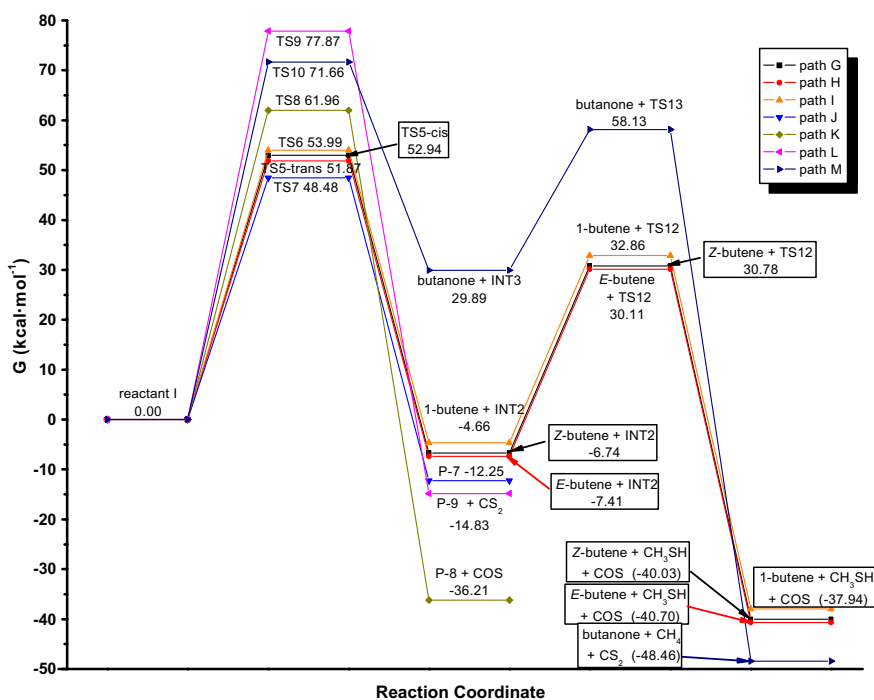
Fig. 2.   Gibbs energy profile of pathways G to M for the pyrolysis of O-*sec*-butyl S-methyl xanthate.

TS9 (77.87 kcal·mol^{-1}) generated P-8 and P-9. The five-membered ring transition state (TS10) had activation energy as high as 71.66 kcal·mol^{-1}, giving butanone and INT3. INT3 decomposed into methane and carbon disulfide *via* TS13 (28.24 kcal·mol^{-1}) with an exothermicity of 37.94 kcal·mol^{-1}.

3.2. *Pyrolysis of S-sec-butyl O-methyl xanthate*

Similar to the thermal decomposition of O-*sec*-butyl S-methyl xanthate, the mechanisms for the pyrolysis of S-*sec*-butyl O-methyl xanthate were displayed in Schemes 5 and 6. Table 2 collected the corrected Gibbs energies for the reactants, transition states and products involved in the pyrolysis of S-*sec*-butyl O-methyl xanthate at MP2/6-31+G(d,p)//MP2/6-31G(d) level, while the detailed electronic energies, zero-point vibrational energies, thermal corrections to enthalpies, entropies and the calculation methods were listed in Table S2 in the supporting information. Meanwhile, Figs. 3 and 4 displayed the free energy profiles for all pathways.

About 13 possible pathways were also found for the thermal decomposition of S-*sec*-butyl O-methyl xanthate. For pathways A′ to I′, Z-butene (for pathways A′, C′ and G′), E-butene (for pathways B′, D′ and H′) and 1-butene (for pathways C′ F′ and I′) were obtained, together with same by-products, methanol and carbon disulfide. Pathway J' underwent a thion-ether to thiol-carbonyl rearrangement, giving
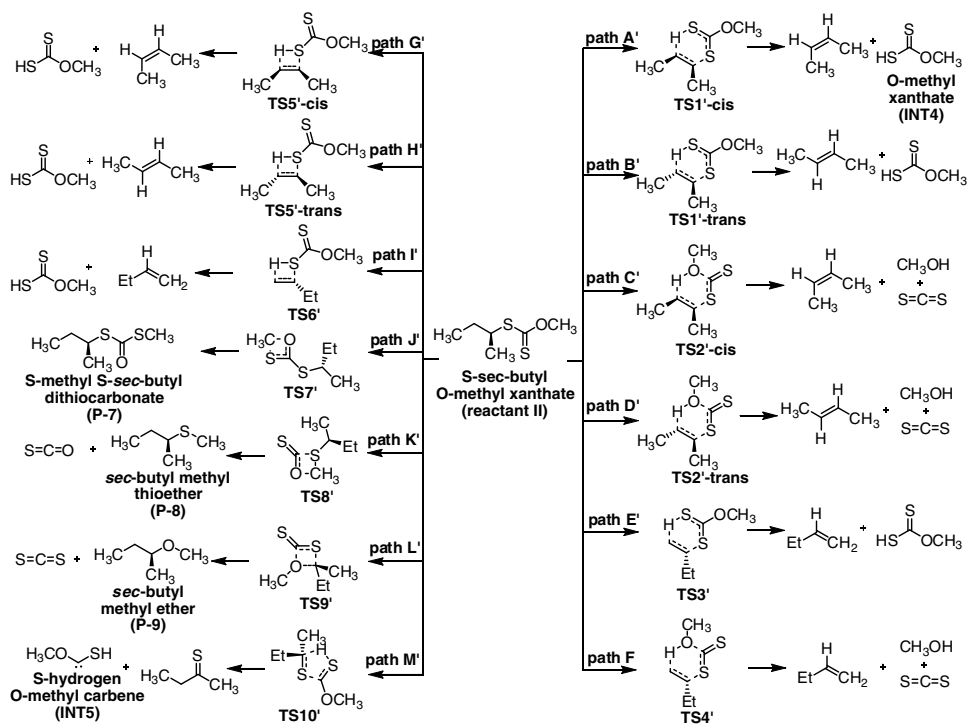
Scheme 5.   13 possible pathways for the pyrolysis of S-*sec*-butyl O-methyl xanthate.
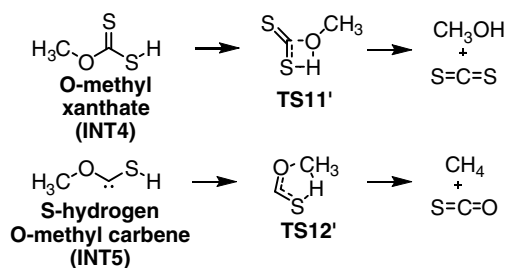

Scheme 6.   Thermal decomposition of INT4 and INT5.

S-methyl S-*sec*-butyl dithiocarbonate (P-7). Pathways K′ and L′ resulted in *sec*-butyl methyl thioether and *sec*-butyl methyl ether with the emission of carbonyl sulfide and carbon disulfide. Pathway M′ passed through a five-membered ring transition state, giving butane-2-thione and S-hydrogen O-methyl carbene (INT5), which decomposed into methane and carbonyl sulfide.

As depicted in Figs. 3 and 4, the lowest six transition states were TS1′-trans (42.65 kcal·mol^{-1}), TS1′-cis (44.00 kcal·mol^{-1}), TS5′-cis (46.04 kcal·mol^{-1}), TS5′-trans (46.08 kcal·mol^{-1}), TS3′ (46.18 kcal·mol^{-1}) and TS6′ (47.08 kcal·mol^{-1}). It

Table 2. Corrected Gibbs energies, in Hartrees, for the reactants, transition states and products involved in the pyrolysis of S-*sec*-butyl O-methyl xanthate at MP2/6-31+G(d,p)//MP2/6-31G(d).

Species	Corrected G	Species	Corrected G	Species	Corrected G
reactant II	−1105.3281974	TS7′	−1105.2447600	P-8	−594.6560415
TS1′-cis	−1105.2580784	TS8′	−1105.2180214	P-9	−272.0430996
TS1′-trans	−1105.2602262	TS9′	−1105.2190422	INT4	−948.6712764
TS2′-cis	−1105.2278313	TS10′	−1105.2163551	INT5	−550.9532339
TS2′-trans	−1105.2287505	TS11′	−948.6144155	CH_3OH	−115.3972433
TS3′	−1105.2545976	TS12′	−550.9079445	CH_4	−40.3634193
TS4′	−1105.2267838	*Z*-butene	−156.6593760	S=C=S	−833.3169485
TS5′-cis	−1105.2548272	*E*-butene	−156.6596631	O=C=S	−510.7380868
TS5′-trans	−1105.2547608	1-butene	−156.6568291	butane-1-thione	−554.3133414
TS6′	−1105.2531660	P-7	−1105.3559477		

should be mentioned that TS5′-cis, TS5′-trans and TS6′ had much lower energy barriers as compared with TS2′-cis (62.98 kcal·mol^{-1}), TS2′-trans (62.40 kcal·mol^{-1}) and TS4′ (63.64 kcal·mol^{-1}), which was different from TS5-cis, TS5-trans and TS6 in the pyrolysis of O-*sec*-butyl S-methyl xanthate. This could be attributed to the atomic sizes of different nucleophiles. Sulfur had a much larger atomic size than oxygen, which could dramatically release the ring strain of the transition states. Both TS1′-trans and TS5′-trans produced E-butene, together with O-methyl
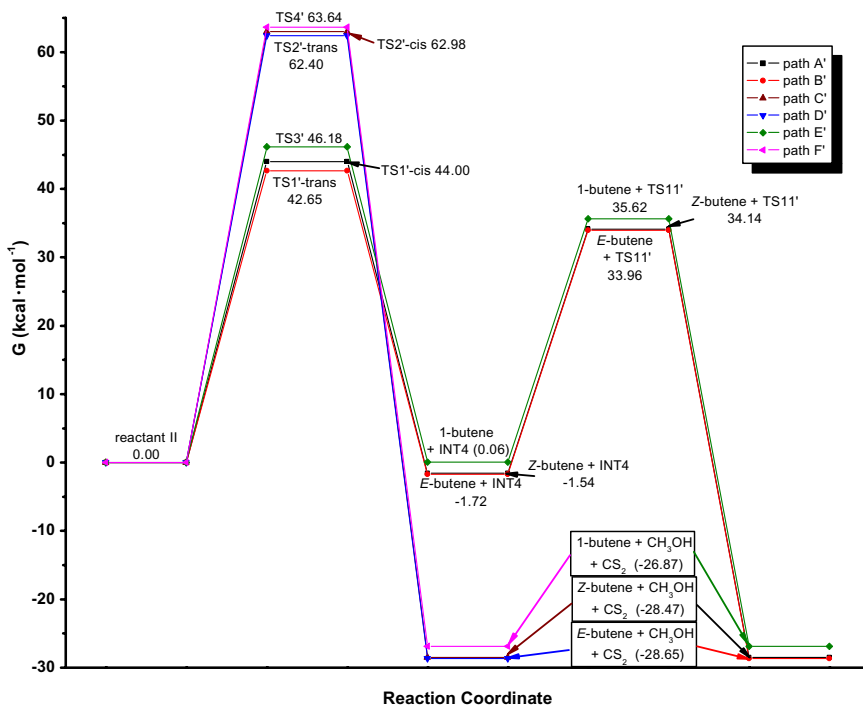
Fig. 3.   Gibbs energy profile of pathways A′ to F′ for the pyrolysis of S-*sec*-butyl O-methyl xanthate.
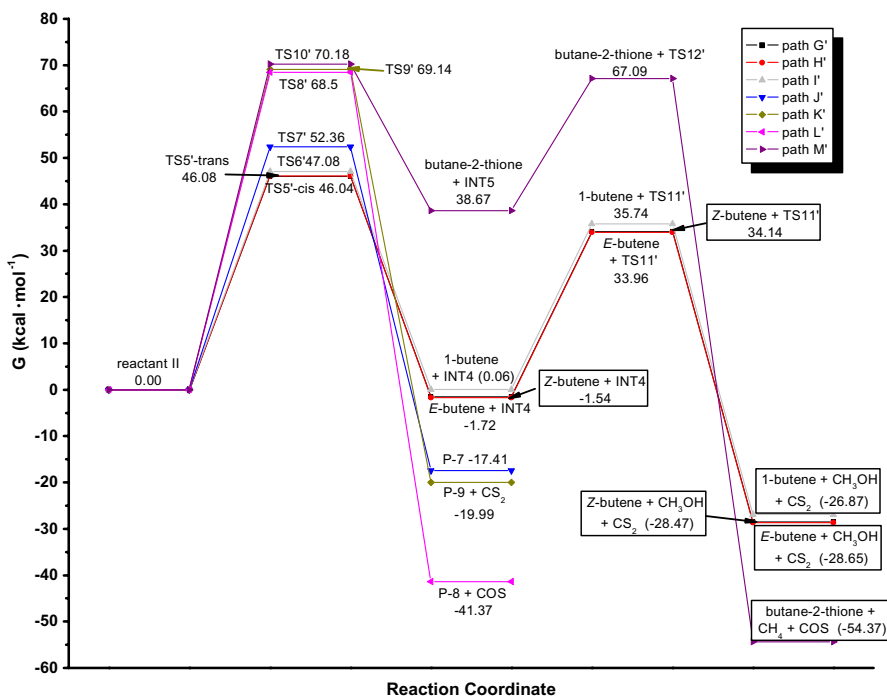
Fig. 4. Gibbs energy profile of pathways G′ to M′ for the pyrolysis of S-*sec*-butyl O-methyl xanthate.

xanthate (INT4), which converted to methanol and carbon disulfide through TS11′ ($35.68 \, \mathrm{kcal \cdot mol^{-1}}$). The final products had exothermicity of $-28.65 \, \mathrm{kcal \cdot mol^{-1}}$ as compared with reactant II. Z-butene could be obtained from TS1′-cis and TS5′-cis, of which TS1′-cis was $1.35 \, \mathrm{kcal \cdot mol^{-1}}$ higher than TS1′-trans and TS5′-cis was slightly lower ($0.04 \, \mathrm{kcal \cdot mol^{-1}}$) than TS5′-trans. The final products were also exothermic of $-28.47 \, \mathrm{kcal \cdot mol^{-1}}$. TS3′ and TS6′ gave 1-butene as the product with activation energies of $46.18 \, \mathrm{kcal \cdot mol^{-1}}$ and $47.08 \, \mathrm{kcal \cdot mol^{-1}}$, which were $3.53 \, \mathrm{kcal \cdot mol^{-1}}$ and $4.43 \, \mathrm{kcal \cdot mol^{-1}}$ higher than TS1′-trans, respectively. The final products were $26.87 \, \mathrm{kcal \cdot mol^{-1}}$ lower than reactant II. As discussed above, E-butene would be collected as the major product with a minor product to be Z-butene, while trace amount of 1-butene could be obtained.

For the rest four mechanisms, TS7′ had an energy barrier of $52.36 \, \mathrm{kcal \cdot mol^{-1}}$, but the rearranged product could give off $69.77 \, \mathrm{kcal \cdot mol^{-1}}$, resulting in an exothermic procedure. The following two transition states (TS8′ and TS9′) had even higher activation energies of $68.50 \, \mathrm{kcal \cdot mol^{-1}}$ and $69.14 \, \mathrm{kcal \cdot mol^{-1}}$, respectively, both of which resulted in the same products as TS8 and TS9. For TS10′, it had the highest activation energy of $70.18 \, \mathrm{kcal \cdot mol^{-1}}$, resulting in butane-2-thione and INT5, which decomposed into methane and carbonyl sulfide *via* TS12′ ($28.42 \, \mathrm{kcal \cdot mol^{-1}}$) with exothermicity of $93.04 \, \mathrm{kcal \cdot mol^{-1}}$, making the total pathway to be $54.37 \, \mathrm{kcal \cdot mol^{-1}}$ lower than reactant II.

4. Conclusion

The pyrolyses of O-*sec*-butyl S-methyl xanthate and S-*sec*-butyl O-methyl xanthate were calculated at the MP2/6-31+G(d,p)//MP2/6-31G(d) level. Thirteen possible pathways were considered for both procedures. In the case of O-*sec*-butyl S-methyl xanthate, the lowest energy pathways, B, A and E, corresponded to the formation of E-butene, Z-butene and 1-butene *via* a two-step mechanism with the first step being a rate-determining step. This theoretical result was consistent with experimental product distribution. As for S-*sec*-butyl O-methyl xanthate, pathways G′, H′ and I′ were found to be favored over pathway E′, which could be attributed to a larger sulfur atomic size than an oxygen atom. Besides, TS3′ and TS6′ were 3.53 kcal·mol^{-1} and 4.43 kcal·mol^{-1} higher than TS1′-trans, which would result in trace amount of 1-butene with E-butene to be a major product and Z-butene as a minor product.

Supplementary Materials

Tables S1 and S2 illustrated the calculated electronic energies, zero-point vibrational energies, thermal corrections to enthalpies, entropies, and the corrected free energies for all species at the level of MP2/6-31+G(d,p)//MP2/6-31G(d). The optimized Cartesian coordinations for all species were collected in Tables S3 and S4. The IRC for all transition states were depicted in Figs. S1-S31.

Acknowledgment

References

1. Tschugaeff L, Ueber eine neue methode zur darstellung ungesättigter kohlenwasserstoffe, *Ber Dtsch Chem Ges* **32**:3332, 1899.
2. Tschugaeff L, Untersuchungen über optische activität, *Ber Dtsch Chem Ges* **31**:1775, 1898.
3. Son S, Dodabalapur A, Lovinger AJ, Galvin ME, Luminescence enhancement by the introduction of disorder into poly(p-phenylene vinylene), *Science* **269**:376, 1995.
4. Son S, Lovinger AJ, Galvin ME, A simple organic-soluble precursor route to PPV for highly efficient and pinhole free led devices, *Polym Mat Sci Eng* **72**:567, 1995.
5. Lo SC, Sheridan AK, Samuel IDW, Burn PL, Comparison of the electronic properties of poly[2-(2′-ethylhexyloxy)-1,4-phenylenevinylene] prepared by different precursor polymer routes, *J Mat Chem* **9**:2165, 1999.
6. Lo SC, Palsson LO, Kilitziraki M, Brun PL, Samuel IDW, Control of polymer–electrode interactions: The effect of leaving group on the optical properties and device characteristics of EHPPV, *J Mat Chem* **11**:2228, 2001.

7. Laue T, Plagens A, *Named Organic Reactions*, 2nd edn., John Wiley & Sons Ltd., Chichester, 2005.

8. Hückel W, Tappe W, Legutke G, Abspaltungsreaktionen und ihr sterischer verlauf, *Ann* **543**:191, 1940.

9. Barton DH, 464. cis-elimination in thermal decomposition, *J Chem Soc* 2174, 1949.

10. Cram DJ, Studies in stereochemistry. IV. The chugaev reaction in the determination of configuration of certain alcohols, *J Am Chem Soc* **71**:3883, 1949.

11. Alexander ER, Mudrak A, Studies on the mechanism of chugaev and acetate thermal decompositions. I. cis- and trans-2-phenylcyclohexanol, *J Am Chem Soc* **72**:1810, 1950.

12. Alexander ER, Mudrak A, Studies on the mechanism of chugaev and acetate thermal decompositions. II. cis- and trans-2-methyl-1-tetralol, *J Am Chem Soc* **72**:3194, 1950.

13. Alexander ER, Mudrak A, Studies on the mechanism of chugaev and acetate thermal decompositions. III. cis- and trans-2-methyl-1-indanol, *J Am Chem Soc* **73**:59, 1951.

14. Bader RFW, Bourns AN, A kinetic isotope effect study of the Tschugaeff reaction, *Can J Chem* **39**:348, 1961.

15. Erickson JA, Kahn SD, Theoretical studies of thermal syn elimination reactions. The relative rates of ethyl formate, ethyl xanthate, and ethyl phosphinate eliminations, *J Am Chem Soc* **116**:6271, 1994.

16. Claes L, Francois JP, Deleuze MS, Theoretical study of the internal elimination reactions of xanthate precursors, *J Comput Chem* **24**:2023, 2003.

17. Harano K, Cascade reactions of unsaturated xanthates and related reactions: Computer-assisted molecular design and analysis of reaction mechanisms, *Yakugaku Zasshi* **125**:469, 2005.

18. Vélez E, Quijano J, Notario R, Murillo J, Ramírez JF, Computational study of the mechanism of thermal decomposition of xanthates in the gas phase (the chugaev reaction), *J Phys Org Chem* **21**:797, 2008.

19. Messaoudi B, Mekelleche SM, Mora-Diez N, Theoretical study of the regioselectivity of the addition of the triplet oxygen atom to unsymmetrical substituted alkenes, *J Theor Comput Chem* **11**:527, 2012.

20. Moeinpour F, Bakavoli M, Davoodnia A, Morsali A, Theoretical and experimental study on the regioselectivity of acrylonitrile and methylmethacrylate 1,3-dipolar cycloaddition to some nitrilimines, *J Theor Comput Chem* **11**:99, 2012.

21. Li Q-G, Xue Y, Ren Y, Wong N-B, Li W-K, *Ab initio* computational investigations on the gas-phase homodimerization and keto-enol tautomerism of the monochalcogenocarboxylic acids $CH_3C(=O)XH$ (X = S, Se, Te), *J Theor Comput Chem* **10**:41, 2011.

22. Yang J, Su K, Liu Y, Wang Y, Zeng Q, Cheng L, Zhang L, New reaction pathways of propene + BCl_3 decomposition in chemical vapor deposition process, *J Theor Comput Chem* **11**:53, 2012.

23. Deka RP, Medhi C, Density functional study on the proton assisted isomerization of 1H-imidazo(4,5-b)pyridine derivatives, *J Theor Comput Chem* **11**:651, 2012.

24. Ditchfield R, Hehre WJ, Pople JA, Self-consistent molecular-orbital methods. IX. An extended Gaussian-type basis for molecular-orbital studies of organic molecules, *J Chem Phys* **54**:724, 1971.

25. Trucks MJ, Schlegel GW, Scuseria HB *et al.*, Gaussian 03, Revision B.03, Gaussian, Inc. Pittsburgh, PA, 2003.

26. Møller C, Plesset M, Note on an approximation treatment for many-electron systems, *Phys Rev* **46**:618, 1934.

27. DePuy CH, Bishop A, Goeders CN, Pyrolytic cis eliminations: The pyrolysis of sec-butyl derivatives, *J Am Chem Soc* **83**:2151, 1961.

28. Scott PA, Radom L, Harmonic vibrational frequencies: An evaluation of Hartree−Fock, Møller−Plesset, quadratic configuration interaction, density functional theory, and semiempirical scale factors, *J Phys Chem* **100**:16502, 1996.
29. Fukui K, Formulation of the reaction coordinate, *J Phys Chem* **74**:4161, 1970.
30. Glasstone KJ, Laidler KJ, Eyring H, *The Theory of Rate Processes*, McGraw-Hill, New York, 1941.
31. Benson SW, *The Foundations of Chemical Kinetics*, McGraw-Hill, New York, 1969.